# Observation and Symmetry-Based Coherent Control of Transient Two-Photon Absorption: The Bright Side of Dark Pulses

Andrey Gandman,* Leonid Rybak, and Zohar Amitay†
*The Shirlee Jacobs Femtosecond Laser Research Laboratory, Schulich Faculty of Chemistry, Technion-Israel Institute of Technology, Haifa 32000, Israel*

(Received 29 June 2013; published 23 July 2014)

We present and experimentally demonstrate for the first time the observation and femtosecond coherent control over the temporal evolution of a transient population that is excited via nonresonant two-photon absorption. Based on symmetry properties of the two-photon absorption process, the exciting femtosecond pulses are phase-shaped to photoinduce different evolutions of the transient excited population for a given final excited population. As a study case, we focus here on the attractive case of two-photon dark pulses that, although inducing zero final population (hence, the terminology of "dark pulses"), they induce a transient excited population during the pulse irradiation that can significantly deviate from zero. This nonzero transient population can be viewed as the bright side of such dark pulses. The symmetry-based coherent control is demonstrated first with dark pulses that we shape to induce transient excited population that at all times is kept below different target levels. Then, it is further demonstrated with pairs of dark pulses where one is rationally shaped to induce temporal evolution of the transient excited population that is the inverse of the evolution induced by the other. The work is conducted in the weak-field regime with the sodium atom as the model system. The approach developed here is general, conceptually simple, and very effective.

DOI: 10.1103/PhysRevLett.113.043003 PACS numbers: 32.80.Qk, 32.80.Wr, 42.65.Re

The general concept of femtosecond quantum coherent control is to control the photoinduced dynamics of a quantum system by utilizing and manipulating interferences among a manifold of coherent excitation pathways that are induced by a broadband femtosecond pulse [1–6]. The control tool is the optical shaping of the pulse [7]. Over the past 20 years, such femtosecond control has been demonstrated very successfully in the lab with many physical systems and various photoprocesses [3–6]. However, except for very few works, all the corresponding studies have focused only on the final outcome of the photoinduced process, and have not been concerned with the exact temporal evolution of the system during the pulse irradiation that leads to the desired outcome. Simultaneous control over both objectives, i.e., the final outcome as well as the exact temporal evolution toward the outcome, can actually be considered as complete quantum coherent control, and its experimental study is of major importance to fundamentals of coherent control and control landscapes. It is also very important for achieving effective coherent control when fast relaxation processes compete with the controlled photoexcitation by either fast depopulation or dephasing of the intermediate or final excitation states. As always, additional important aspects and applications might arise as progress will be made in this direction of complete dynamical quantum control. The few relevant experimental studies that have previously been conducted include the observation [8] and control [9,10] of coherent transients in one-photon excitation of a two-level atomic system, and their utilization for time-resolved quantum state holography [11], femtosecond spectral electric field reconstruction [12], and high-precision calibration of pulse-shaping setups [13]. No experimental work has previously studied coherent control of temporal evolution in two-photon excitation or any other multiphoton excitation.

In this Letter, we present and experimentally demonstrate for the first time femtosecond coherent control over the temporal evolution of a transient population that is excited via nonresonant two-photon absorption. Based on symmetry properties of the two-photon absorption process, utilizing the invariance of the final excited population to specific phase transformations of the exciting pulse [14], the exciting femtosecond pulses are phase shaped to photoinduce different evolutions of the transient excited population for a given final excited population. The framework of the demonstrated scheme extends the weak-field frequency-domain two-photon control picture, used so far for analyzing the final excited population after the pulse ends [15], to also describe the time-dependent evolution of the excited population during the pulse irradiation. As a study case, we focus here on the attractive case of two-photon dark pulses that, while inducing zero final population, they can induce a significant nonzero transient excited population during the pulse irradiation. This nonzero transient population can be viewed as the bright side of such dark pulses. We first demonstrate the symmetry-based coherent control with dark pulses that we

 

shape to induce a transient excited population that at all times is kept below different target levels. Then, the control is further demonstrated with pairs of dark pulses where one is rationally shaped to induce temporal evolution of the transient excited population that is the inverse of the evolution induced by the other. The approach developed here is general, conceptually simple, and very effective.

We consider a nonresonant two-photon absorption process from an initial state $|g\rangle$ to a final state $|f\rangle$ that is induced by a weak shaped femtosecond pulse of the temporal field $\epsilon(t)$. The initial and final states are coupled via a manifold of intermediate states $|n\rangle$ that are all far from resonance with the exciting pulse. Based on second-order perturbation theory [5,6], the transient amplitude $A_f(t)$ of $|f\rangle$ at time $t$ is given in the time domain as

$$A_f(t) = -\frac{1}{\hbar^2}\sum_n \mu_{fn}\mu_{ng}\int_{-\infty}^{t}\int_{-\infty}^{t_1}\varepsilon(t_1)\varepsilon(t_2)\exp[i(\omega_{fn}t_1+\omega_{ng}t_2)]dt_1dt_2, \quad (1)$$

and in the frequency domain as

$$A_f(t) = \frac{\mu_{fg}^2}{2\pi i\hbar^2}\int_{-\infty}^{\infty}\int_{-\infty}^{\infty}\frac{E(\omega)E(\omega')}{\omega_{fg}-(\omega+\omega')}\exp\{i[\omega_{fg}-(\omega+\omega')]t\}d\omega d\omega', \quad (2)$$

where $\omega_{ij}$ and $\mu_{ij}$ are, respectively, the transition frequency and dipole matrix element between a pair of states, and $\mu_{fg}^2$ is the effective $|f\rangle$-$|g\rangle$ two-photon coupling. $E(\omega) \equiv |E(\omega)|\exp[i\Phi(\omega)]$ is the pulse's spectral field, which is related to $\epsilon(t)$ via Fourier transform, with $|E(\omega)|$ and $\Phi(\omega)$ being the spectral amplitude and phase at frequency $\omega$. For the (unshaped) transform-limited (TL) pulse, $\Phi(\omega) = 0$. Following further development,

$$A_f(t) = \frac{\mu_{fg}^2}{2\pi i\hbar^2}[A_{\text{on-res}} + A_{\text{near-res}}(t)], \quad (3)$$

with the on-resonant part

$$A_{\text{on-res}} = i\pi A^{(2)}(\omega_{fg}), \quad (4)$$

and the near-resonant part

$$A_{\text{near-res}}(t) = -\wp\int_{-\infty}^{\infty}\frac{1}{\delta}A^{(2)}(\omega_{fg}-\delta)\exp(-i\delta t)d\delta, \quad (5)$$

where $A^{(2)}(\Omega) = \int_{-\infty}^{\infty}E(\omega)E(\Omega-\omega)d\omega$, and $\wp$ indicates the Cauchy's principal value. The transient population of $|f\rangle$ is $P_f(t)=|A_f(t)|^2$. At times after the pulse ends, $A_{\text{near-res}}(t\to\infty)=A_{\text{on-res}}$ and, thus, $A_{f,\text{outcome}} \equiv A_f(t\to\infty) \propto A_{\text{on-res}} \propto A^{(2)}(\omega_{fg})$. Hence, the final excited population is $P_{f,\text{outcome}} \equiv P_f(t\to\infty) = |A_{f,\text{outcome}}|^2 \propto |A_{\text{on-res}}|^2 \propto |A^{(2)}(\omega_{fg})|^2$. So, based on the above frequency-domain formulation, one obtains that $P_f(t)$ results from all the two-photon pathways, which are either on- or near-resonance with $|f\rangle$, while $P_{f,\text{outcome}}$ results only from the on-resonant pathways (see Fig. 1).

Our present objective is to coherently control the transient population $P_f(t)$ and its time dependence, while keeping the final population $P_{f,\text{outcome}}$ on a preset value. This stands for the simultaneous control over both the final outcome and the exact temporal evolution toward this outcome. In order to achieve this goal, we utilize transformations $\hat{U}^{\text{transient}}$ of the spectral field $E(\omega)$ that do not change $P_{f,\text{outcome}}$ but do change the transient time dependence of $P_f(t)$. This invariance of the nonresonant two-photon absorption process is the symmetry property that we exploit [14]. Based on Eqs. (3)–(5), it applies to any phase transformation $\hat{U}^{\text{transient}} = \exp[i\Phi^{(\text{add})}_{\text{antisym}}(\omega)]$ that keeps $|E(\omega)|$ unchanged while adding to $\Phi(\omega)$ a $\Phi^{(\text{add})}_{\text{antisym}}(\omega)$ that is antisymmetric around $\omega_{fg}/2$, i.e.,

$$\Phi^{(\text{add})}_{\text{antisym}}(\omega_{fg}/2+\beta) - \Phi^{(\text{add})}_{\text{antisym}}(\omega_{fg}/2) = -[\Phi^{(\text{add})}_{\text{antisym}}(\omega_{fg}/2-\beta) - \Phi^{(\text{add})}_{\text{antisym}}(\omega_{fg}/2)], \quad (6)$$

for any value of $\beta$.

Hence, the following new symmetry-based coherent control scheme for designing the spectral phase pattern

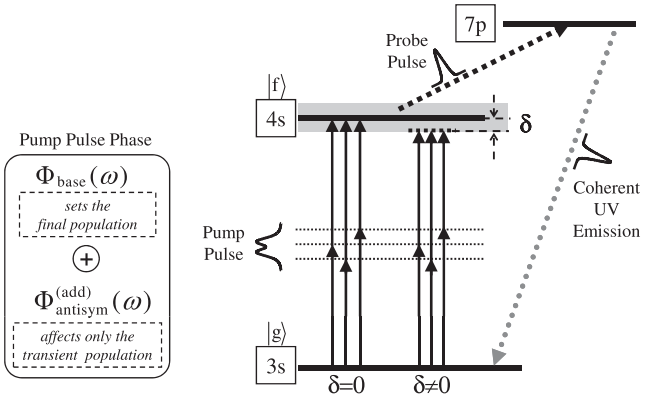


FIG. 1. The excitation scheme of Na for the study of symmetry-based coherent control of transient two-photon absorption.

$\Phi(\omega)$ is introduced here. The final excited population $P_{f,\mathrm{outcome}}$ is set to a chosen value $P^{(\mathrm{base})}_{f,\mathrm{outcome}}$ by choosing a proper base phase pattern $\Phi^{(\mathrm{base})}(\omega)$. The corresponding value of $P_{f,\mathrm{outcome}}$ is the value photoinduced by a reference shaped pulse having $\Phi(\omega) = \Phi^{(\mathrm{base})}(\omega)$. Then, by adding different suitable antisymmetric phase patterns $\Phi^{(\mathrm{add})}_{\mathrm{antisym}}(\omega)$, the temporal evolution of the transient excited population $P_f(t)$ during the pulse irradiation is modified, while the outcome is kept constant on $P^{(\mathrm{base})}_{f,\mathrm{outcome}}$. The total phase pattern applied to the shaped pulse is $\Phi(\omega) = \Phi^{(\mathrm{base})}(\omega) + \Phi^{(\mathrm{add})}_{\mathrm{antisym}}(\omega)$. Since $\Phi^{(\mathrm{base})}(\omega)$ can generally be any chosen phase pattern, $\Phi(\omega)$ is generally not antisymmetric around $\omega_{fg}/2$.

The present model system is the sodium atom (Fig. 1), with the $3s$ ground state as $|g\rangle$ and $4s$ excited state as $|f\rangle$, where $\omega_{fg}$ corresponds to two 777-nm photons. The nonresonant two-photon absorption process is induced by a phase-shaped linearly polarized femtosecond pump pulse whose shape controls both the final and transient $4s$ population. It is of about 777-nm central wavelength, 4 nm bandwidth, 200-fs TL duration, and $5 \times 10^9 - \mathrm{W/cm^2}$ TL peak intensity. The time-dependent $4s$ population is probed using a time-delayed probe pulse that is much shorter and weaker than the pump pulse. It induces a one-photon absorption transition to the $7p$ state ($\omega_{7p,4s}$ corresponds to a 781.2-nm photon), which is followed by an emission of a coherent UV radiation at $\omega_{7p,3s}$ (corresponding to a 259.5-nm photon) upon stimulated deexcitation to $3s$ [16]. The linearly polarized probe pulse is a TL pulse of 790-nm central wavelength, 12-nm bandwidth, and ~80-fs duration. Its peak intensity is below $10^7$ $\mathrm{W/cm^2}$, such that no significant three-photon excitation to $7p$ and no detectable UV radiation are induced by the probe pulse alone. In order to prevent three-photon resonant access to $7p$ and UV emission by the pump pulse alone, the pump pulse spectrum results from properly blocking an original broader spectrum at its lower-frequency edge. The integrated intensity of the coherent UV emission at $\omega_{7p,3s}$ is proportional to the final population of the $7p$ state [16]. In the present excitation scheme, as the probe pulse is much shorter than the pump pulse, at a given pump-probe delay time $\tau$, the final $7p$ population is proportional to the transient $4s$ population $P_{4s}(\tau)$. So, overall, the integrated intensity of the UV emission is a relative measure of $P_{4s}(\tau)$ and at delay times after the pump pulse ends it corresponds to $P_{4s,\mathrm{outcome}}$. This is corroborated by the results presented below, particularly by the excellent experimental-theoretical agreement that they show. It is worth noting that generally the final $7p$ population, and, hence, also $P_{4s}(\tau)$, can also be obtained by measuring the spontaneous emission from the $7p$ state. Experimentally, sodium vapor in a heated cell with Ar buffer gas is irradiated with such pump and probe laser pulses, after the former undergoes shaping using a liquid-crystal spatial light phase modulator [7]. The forward-emitted coherent UV radiation is measured after the cell. It is worth mentioning that the experimental conditions are such that no detectable UV radiation is generated in the cell via nonresonant four-wave mixing processes.

Figure 2 presents several examples of results for basic phase control of transient two-photon absorption, where different temporal evolutions of the transient population are photoinduced for a given final population outcome. The presented results correspond to two extreme cases of the final outcome: (i) the final outcome is the maximal two-photon absorption and $P_{4s,\mathrm{outcome}} = P^{(\mathrm{max})}_{4s,\mathrm{outcome}}$ [Figs. 2(a)–2(b)], and (ii) the final outcome is zero two-photon absorption and $P_{4s,\mathrm{outcome}} = 0$ [Figs. 2(c)–2(d)]. The shaped pulses inducing the latter are referred to as "two-photon dark pulses" [14,15]. The maximal two-photon absorption refers to the maximal absorption for the present excitation, i.e., for the present spectrum and energy of the pump pulse and the present experimental focusing conditions. The main graphs of the different panels show the experimental (circles) and theoretical (black lines) results of the $4s$ transient population $P_{4s}(\tau)$ as a function of the pump-probe delay time $\tau$ for different shapes of the pump pulse. For controlling the final and transient populations, the corresponding spectral phase patterns are designed along our new symmetry-based scheme. For each case, the two corresponding phase components, the base phase pattern $\Phi^{(\mathrm{base})}(\omega)$ and antisymmetric phase addition $\Phi^{(\mathrm{add})}_{\mathrm{antisym}}(\omega)$, are shown in the panel's inset in blue and red lines, respectively. For completeness, the different panels also show the temporal intensity profile of the different shaped pump pulses (gray

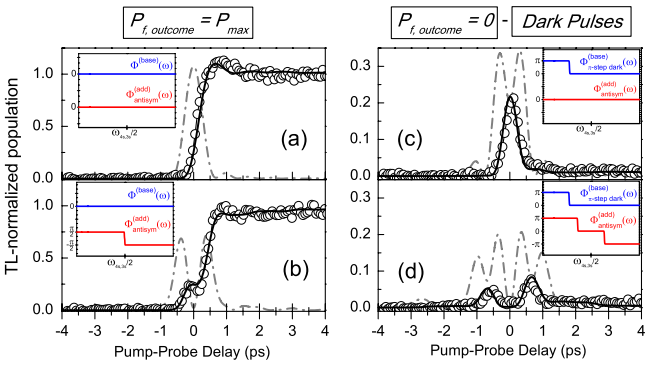


FIG. 2 (color online). Experimental (circles) and calculated (black solid lines) results for basic symmetry-based phase control of transient two-photon absorption. Different temporal evolutions of the $4s$ transient population are photoinduced for a given final population that is (a),(b) maximal, and (c),(d) zero (dark pulses). The components of the spectral phase of the different shaped pulses, the base phase pattern (blue line) and antisymmetric phase addition (red line), are shown in the insets. The temporal intensity of the different pulses (gray dotted-dashed lines) are also shown.

dotted-dashed lines). All the presented traces of $P_{4s}(\tau)$ are normalized by the maximal final population $P^{(\max)}_{4s,\text{outcome}}$ that is induced by the TL pulse [14,15]. The theoretical results are the results of numerical calculations using the frequency-domain formulation of Eqs. (2)–(5) or, equivalently, the time-domain formulation of Eq. (1). As seen, there is an excellent agreement between the experimental and theoretical results, which confirms our correct understanding of the experimental signal and measurements.

Figures 2(a) and 2(b) present results for the above case (i), with two different shaped pump pulses that each photoinduces a different temporal evolution of $P_{4s}(\tau)$ toward the maximal final population $P^{(\max)}_{4s,\text{outcome}}$. For this, the spectral phase patterns of these two shaped pulses are applied with a base phase pattern that is zero $[\Phi^{(\text{base})}(\omega) = 0]$ and different antisymmetric phase additions $\Phi^{(\text{add})}_{\text{antisym}}(\omega)$. For the pulse of Fig. 2(a), $\Phi^{(\text{add})}_{\text{antisym}}(\omega) = 0$ and the total phase pattern is, thus, also zero, and the shaped pump pulse is actually the TL pulse. On the other hand, for the pulse of Fig. 2(b), the antisymmetric phase addition is of a single $\pi$ step located at $\omega = \omega_{4s,3s}/2 = 12\,870.0\ \text{cm}^{-1}$ (777.0 nm), and thus, the total phase pattern is also equal to this $\pi$ phase step.

Figures 2(c) and 2(d) present results for the above case (ii), with two different two-photon dark pulses that each photoinduces a completely different temporal evolution of $P_{4s}(\tau)$ with zero final population. As seen, even though the final population is zero, the transient population during the pulse irradiation can significantly deviate from zero, and the corresponding evolution and upper limit can extensively vary from one case to the other. In the examples of Figs. 2(c) and 2(d), the evolution trace of $P_{4s}(\tau)$ has a structure of either a single or double peak, respectively, and the transient population is always kept below either 25% or 10% of $P^{(\max)}_{4s,\text{outcome}}$, respectively. This overall photoinduced transient behavior adds new dimension to phase control using the family of two-photon dark pulses. For setting the level of zero final population, the spectral phase patterns of the present dark pulses are built with a base phase pattern $\Phi^{(\text{base})}(\omega) = \Phi^{(\text{base})}_{\pi\text{-step,dark}}(\omega)$ that is of a single $\pi$ step at position $\omega = \omega^{(\text{base})}_{\pi\text{-step,dark}} = 12\,884.6\ \text{cm}^{-1}$ (776.12 nm). This value of $\omega^{(\text{base})}_{\pi\text{-step,dark}}$ is set such that the reference shaped pump pulse with $\Phi(\omega) = \Phi^{(\text{base})}_{\pi\text{-step,dark}}(\omega)$ is a two-photon dark pulse for the present two-photon transition [14]. The antisymmetric phase additions of the present dark pulses are as follows. For the dark pulse inducing the evolution shown in Fig. 2(c), the phase addition is zero. The corresponding total phase pattern is, thus, of a $\pi$ step at $\omega^{(\text{base})}_{\pi\text{-step,dark}}$. On the other hand, for the dark pulse inducing the other (completely different) evolution shown in Fig. 2(d), the antisymmetric phase addition is composed of two phase steps that are positioned symmetrically around $\omega_{4s,3s}/2 = 12\,870.0\ \text{cm}^{-1}$ at offsets of $\pm 8.9\ \text{cm}^{-1}$. The resulting total phase pattern is, thus, composed here of several phase steps at different positions.

Next, we demonstrate a more sophisticated symmetry-based coherent control of transient two-photon absorption with the attractive family of two-photon dark pulses. In this part of the study, pairs of dark pulses are rationally phase-shaped to induce time-inverted transient evolutions of the excited population; i.e., one pulse is shaped to induce a time-dependent evolution that is the inverse of the evolution induced by the other. The corresponding scheme utilizes the effect of applying the sign-inversion phase transformation, $\hat{U}^{\text{phase-sign-inversion}}: |E(\omega)| \exp[i\Phi(\omega)] \rightarrow |E(\omega)| \exp[-i\Phi(\omega)]$, to the spectral field $E(\omega)$. Based on the equations above, it leads to $A^{(2)}(\Omega) \rightarrow [A^{(2)}(\Omega)]^*$ and $A_{\text{near-res}}(t) \rightarrow [A_{\text{near-res}}(-t)]^*$. For a two-photon dark pulse, $P^{\text{dark}}_{f,\text{outcome}} = 0$ as well as $A^{\text{dark}}_{\text{on-res}} = 0$, where the latter originates from the general relation of $P_{f,\text{outcome}} \propto |A_{\text{on-res}}|^2$ (see above). So, based on Eq. (3), it is also obtained for a two-photon dark pulse that $A^{\text{dark}}_f(t) \propto A^{\text{dark}}_{\text{near-res}}(t)$. Hence, overall, the application of the sign-inversion phase transformation to the field of a two-photon dark pulse leads to $A^{\text{dark}}_f(t) \rightarrow [A^{\text{dark}}_f(-t)]^*$ and $P^{\text{dark}}_f(t) \rightarrow P^{\text{dark}}_f(-t)$. In other words, any pair of dark pulses (labeled as 1 and 2) that have the same spectral amplitude ($|E(\omega)|$) and their total spectral phases, $\Phi_1$ and $\Phi_2$, satisfy the sign-inversion relation, $\exp[i\Phi_1(\omega)] = \exp[-i\Phi_2(\omega)]$, induce transient evolutions of the excited population that are time inverted.

In the present corresponding experiments, the spectral phase $\Phi(\omega)$ of different shaped dark pulses is designed based on our new symmetry-based scheme, and then, the control objective of time inversion is achieved by applying the sign inversion to their spectral phase. The zero final population is set here for all the dark pulses by applying $\Phi^{(\text{base})}(\omega) = \Phi^{(\text{base})}_{\pi\text{-step,dark}}(\omega)$ (see above). Then, for inducing the different temporal evolutions by the different dark pulses, we choose here antisymmetric phase additions, which are of the cubic form $\Phi^{(\text{add})}_{\text{antisym,cubic}}(\omega; \phi^{(\text{add})}_3) = \frac{1}{6}\phi^{(\text{add})}_3(\omega - \omega_{4s,3s}/2)^3$ characterized by the $\phi^{(\text{add})}_3$ value. So, the corresponding total phase patterns $\Phi(\omega)$ are of the form $\Phi_{\text{dark}}(\omega; \phi^{(\text{add})}_3) = \Phi^{(\text{base})}_{\pi\text{-step,dark}}(\omega) + \frac{1}{6}\phi^{(\text{add})}_3(\omega - \omega_{4s,3s}/2)^3$, and the sign-inversion relation $\exp[i\Phi_{\text{dark}}(\omega; \phi^{(\text{add})}_3)] = \exp[-i\Phi_{\text{dark}}(\omega; -\phi^{(\text{add})}_3)]$ holds for them. Hence, the evolution induced by a dark pulse having a spectral phase with $\phi^{(\text{add})}_3$ is time inverted by a dark pulse that is shaped to have a spectral phase with $-\phi^{(\text{add})}_3$.

Figure 3 shows the time-inversion experimental results. In the figure, each row of panels corresponds to a different pair of shaped dark pulses that induce time-inverted

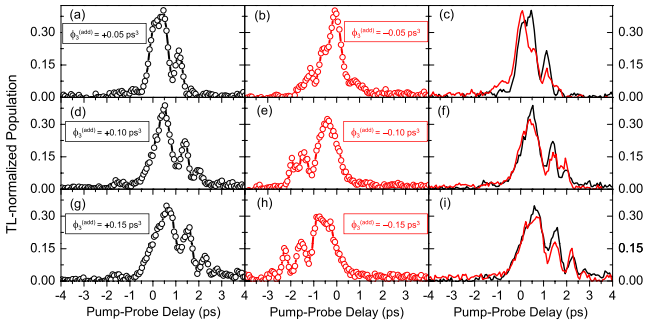


FIG. 3 (color online). Experimental results for time-inversion symmetry-based transient coherent control with pairs of two-photon dark pulses that photoinduce time-inverted evolutions of the 4*s* transient population. Each row corresponds to a different pair of dark pulses: the induced traces are presented individually in the first two panels of each row [(a),(b), (d),(e), and (g),(h)], while the third panel of each row [(c), (f), and (i)] compares them by presenting the first one as is (black line) and the second one after its numerical time-inversion (red line). See text for details.

transient evolutions of $P_{4s}(\tau)$. In the first row, Figs. 3(a) and 3(b) present the traces corresponding to the pulses with $\phi_3^{(\mathrm{add})} = +0.05\ \mathrm{ps}^3$ (black color) and $-0.05\ \mathrm{ps}^3$ (red color), respectively. To clearly illustrate the demonstrated time inversion, Fig. 3(c) compares these two traces by presenting the former one as is (black line) and the latter one after its numerical time inversion (red line). The numerically time-inverted trace of a given trace $P_{4s}(\tau)$ is $P_{4s}^{(\mathrm{inverted})}(\tau) = P_{4s}(-\tau)$. Similarly, in the second row, Figs. 3(d) and 3(e) present the traces for the pair of dark pulses with $\phi_3^{(\mathrm{add})} = \pm 0.10\ \mathrm{ps}^3$ and Fig. 3(f) compares them, while Figs. 3(g) and 3(h) of the third row display the traces for pulses with $\phi_3^{(\mathrm{add})} = \pm 0.15\ \mathrm{ps}^3$ and Fig. 3(i) presents their comparison. As seen, in all the cases [Figs. 3(c), 3(f), and 3(i)], the compared traces experimentally agree well one with the other. Hence, for all the different dark pulses, the experimental results, indeed, clearly demonstrate the desired coherent control of time inverting the evolution of the transient excited population, while keeping the final excited population zero. The complete set of results also demonstrates the robustness of the corresponding transient coherent control.

In conclusion, observation and symmetry-based femtosecond coherent control of transient two-photon absorption is experimentally demonstrated for the first time. The time evolution of the transient excited population (during the pulse irradiation) is controlled independently of the final excited population (after the pulse end). The present study case is the attractive family of two-photon dark pulses. The approach presented here for the corresponding symmetry-based pulse design is general, conceptually simple, and very effective. It can be applied to any system once its symmetry properties are identified.

A. G. and L. R. contributed equally to this work. This research was supported by the Israel Science Foundation (Grant No. 1450/10) and the James Franck Program in Light Matter Interaction.

*Current address: Department of Chemistry, University of California, Berkeley, California 94720, USA
†amitayz@tx.technion.ac.il

[1] D. J. Tannor, R. Kosloff, and S. A. Rice, J. Chem. Phys. **85**, 5805 (1986).
[2] M. Shapiro and P. Brumer, *Principles of the Quantum Control of Molecular Processes* (Wiley, New Jersey, 2003).
[3] H. Rabitz, R. de Vivie-Riedle, M. Motzkus, and K. Kompa, Science **288**, 824 (2000).
[4] T. Brixner and G. Gerber, ChemPhysChem **4**, 418 (2003).
[5] M. Dantus and V. V. Lozovoy, Chem. Rev. **104**, 1813 (2004); ChemPhysChem **6**, 1970 (2005).
[6] Y. Silberberg, Annu. Rev. Phys. Chem. **60**, 277 (2009).
[7] A. M. Weiner, Rev. Sci. Instrum. **71**, 1929 (2000); T. Brixner and G. Gerber, Opt. Lett. **26**, 557 (2001); T. Brixner, G. Krampert, P. Niklaus, and G. Gerber, Appl. Phys. B **74**, S133 (2002).
[8] S. Zamith, J. Degert, S. Stock, B. de Beauvoir, V. Blanchet, M. Aziz Bouchene, and B. Girard, Phys. Rev. Lett. **87**, 033001 (2001).
[9] J. Degert, W. Wohlleben, B. Chatel, M. Motzkus, and B. Girard, Phys. Rev. Lett. **89**, 203003 (2002).
[10] N. Dudovich, D. Oron, and Y. Silberberg, Phys. Rev. Lett. **88**, 123004 (2002).
[11] A. Monmayrant, B. Chatel, and B. Girard, Phys. Rev. Lett. **96**, 103002 (2006).
[12] A. Monmayrant, B. Chatel, and B. Girard, Opt. Lett. **31**, 410 (2006).
[13] W. Wohlleben, J. Degert, A. Monmayrant, B. Chatel, M. Motzkus, and B. Girard, Appl. Phys. B **79**, 435 (2004).
[14] Z. Amitay, A. Gandman, L. Chuntonov, and L. Rybak, Phys. Rev. Lett. **100**, 193002 (2008).
[15] D. Meshulach and Y. Silberberg, Nature (London) **396**, 239 (1998); Phys. Rev. A **60**, 1287 (1999).
[16] L. Rybak, L. Chuntonov, A. Gandman, N. Shakour, and Z. Amitay, Opt. Express **16**, 21738 (2008).